SRR-CWDA-2021-00052

July 26, 2021

To: K. H. Rosenberger, 705-1C

From: G. P. Flach, 705-1C GREGORY FLACH (Affiliate) Digitally signed by GREGORY FLACH (Affiliate) Date: 2021.07.26 08:34:04 -04'00'

Reviewer: S. P. Hommel, 705-1C Steven Hommel Digitally signed by Steven Hommel Date: 2021.07.26 08:46:47 -04'00'

Supplemental Information and Proposed Probabilistic Inputs Related to NRC RSI-4: Saltstone Degradation

Following a preliminary review of the SDF PA, the Nuclear Regulatory Commission (NRC) requested supplemental information regarding physical degradation of saltstone. This Request for Supplemental Information (RSI) is denoted *RSI-4: Saltstone Degradation* (NRC 2020) and reproduced in the Appendix. This memorandum provides supplemental information on mechanisms that could degrade saltstone besides decalcification and proposes statistical distributions for components of a generalized saltstone degradation model to support probabilistic sensitivity analysis and uncertainty quantification under *RSI-1: Combined Uncertainty of Flow Barriers*.

Sulfate attack: SRNL-STI-2014-00397 prepared unary, binary, and ternary dry-component grout samples involving cement, slag, and/or fly ash mixed with water or 4.4 M sodium salt solution. Samples were cured for 2 or 14 months after which crystalline phases were characterized using X-ray powder diffraction. Neither ettringite nor gypsum were detected in the cement + slag + fly ash + salt solution samples for either curing duration (Table 10 of SRNL-STI-2014-00397).

These experimental observations are supported by chemical equilibrium modeling using PHREEQC (version 3.6.2, https://www.usgs.gov/software/phreeqc-version-3) and the CEMDATA18.1 thermodynamic database (Lothenbach et al. 2019). Equilibrium chemistry simulations for this study are based on SRR-CWDA-2021-00034 with two enhancements. First, the sodium-bearing components of the CNASH solid solution model (INFCN, INFCNA, 5CNA) are included because salt solution contains significant amounts of sodium, unlike hydrated waste tank fill grout considered in SRR-CWDA-2021-00034. Second, half of the simulations invoke the "SOLID_SOLUTIONS" keyword in PHREEQC whereby the equilibrium constant (K) for a solid solution component is taken as the ion activity product (IAP) for the dissolution reaction divided by its mole fraction (X); otherwise, each component of the solid solution is treated as an independent pure phase using the "EQUILIBRIUM_PHASES" keyword. Following SRR-CWDA-2021-00034, two cases were considered for the degrees of hydration of dry cement, slag, and fly ash: 100/100/100% (complete hydration of dry binders), and 100/70/20% (partial hydration of slag and fly ash). The extended Debye-Hückel activity model associated with CEMDATA18.1 is accurate for ionic strengths to about one molal (Lothenbach et al. 2019). The pore solutions of grouts prepared with salt solution (X-ESR-Z-00045 Table 2-3) have simulated ionic strengths that exceed three molal. Therefore, three variations on the mix solution were considered: SDF salt solution; salt solution except the $NaSO_4$ component diluted to achieve about one molal ionic strength in grout pore solutions; and pure water. In all, 12 combinations of solid solution model (2), degree of hydration (2), and mix fluid (3) were considered, as indicated by Figures 1 through 3.

Figure 1: Mineral evolution for saltstone dry ingredients mixed with <u>salt solution</u>.

a) 100/100/100% hydration + SOLID_SOLUTIONS option

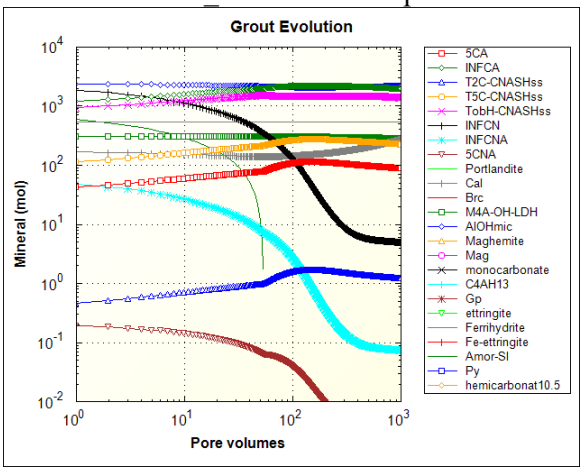

b) 100/100/100% hydration + EQUILIBRIUM_PHASES option

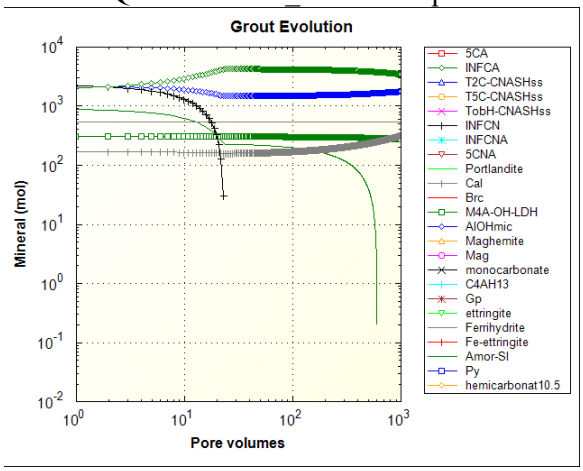

c) 100/70/20% hydration + SOLID_SOLUTIONS option

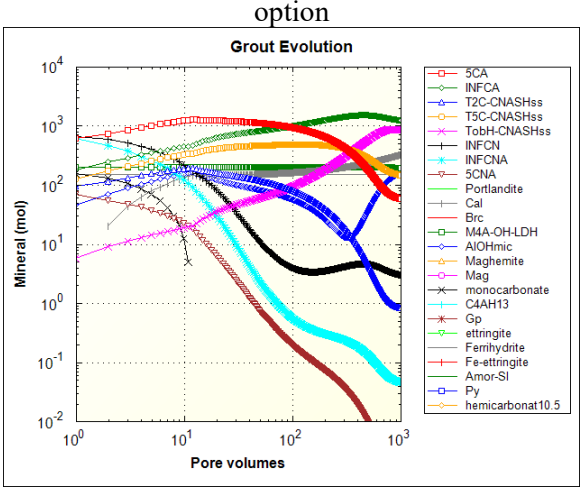

d) 100/70/20% hydration + EQUILIBRIUM_PHASES option

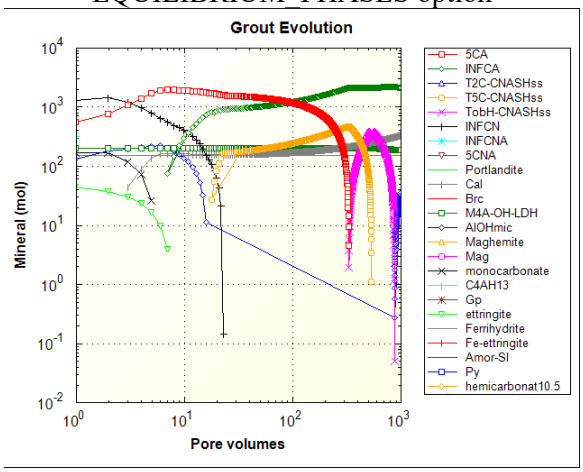

Figure 2: Mineral evolution for saltstone dry ingredients mixed with <u>diluted salt solution</u>.

a) 100/100/100% hydration + SOLID_SOLUTIONS option

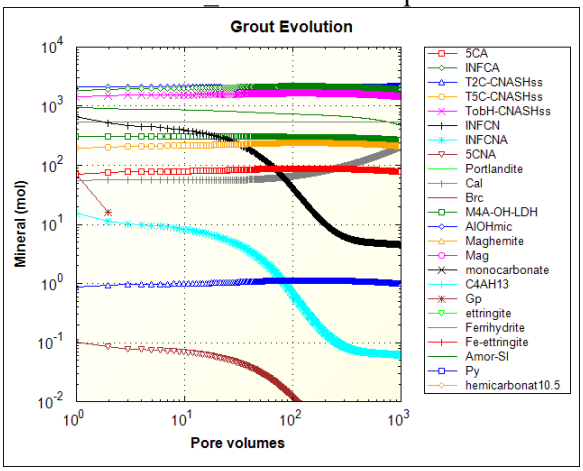

b) 100/100/100% hydration + EQUILIBRIUM_PHASES option

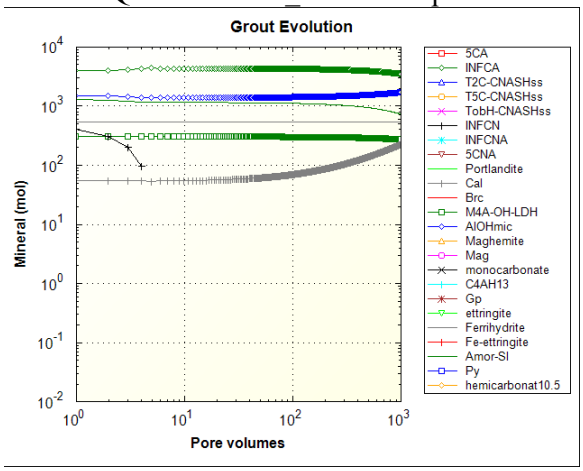

c) 100/70/20% hydration + SOLID_SOLUTIONS option

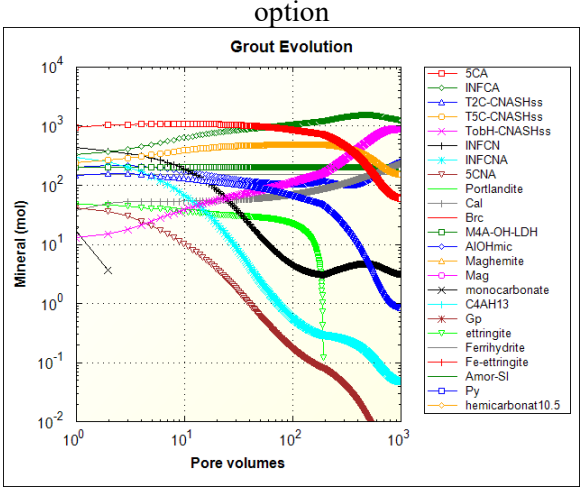

d) 100/70/20% hydration + EQUILIBRIUM_PHASES option

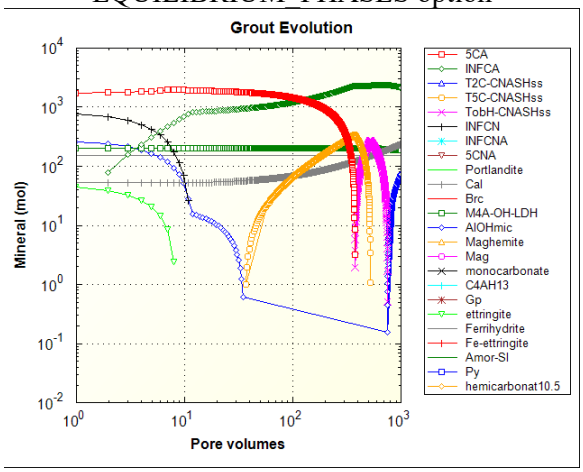

Figure 3: Mineral evolution for saltstone dry ingredients mixed with <u>water</u>.

a) 100/100/100% hydration + SOLID_SOLUTIONS option

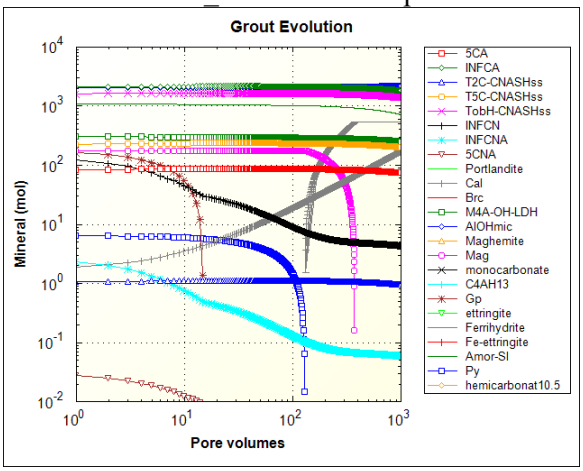

b) 100/100/100% hydration + EQUILIBRIUM_PHASES option

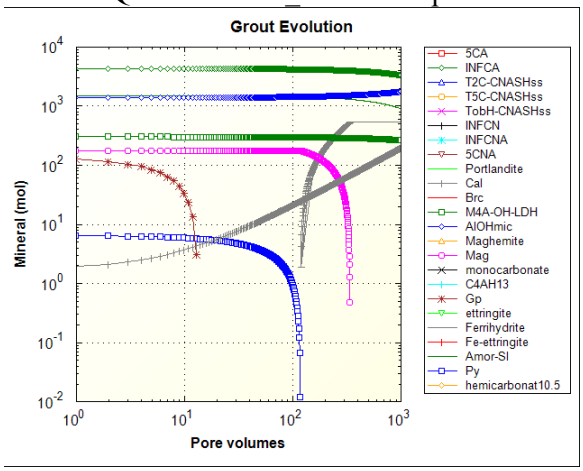

c) 100/70/20% hydration + SOLID_SOLUTIONS option

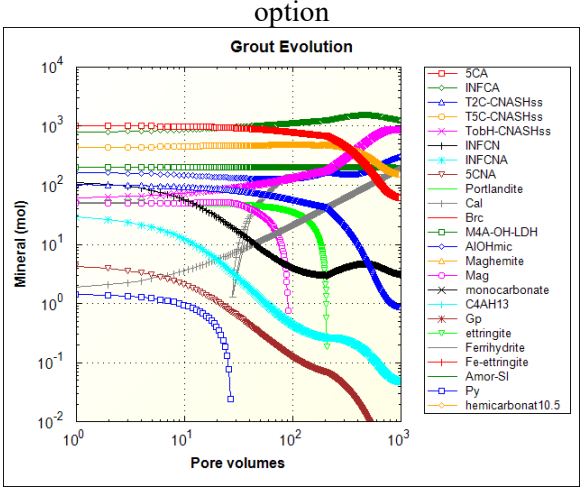

d)100/70/20% hydration + EQUILIBRIUM_PHASES option

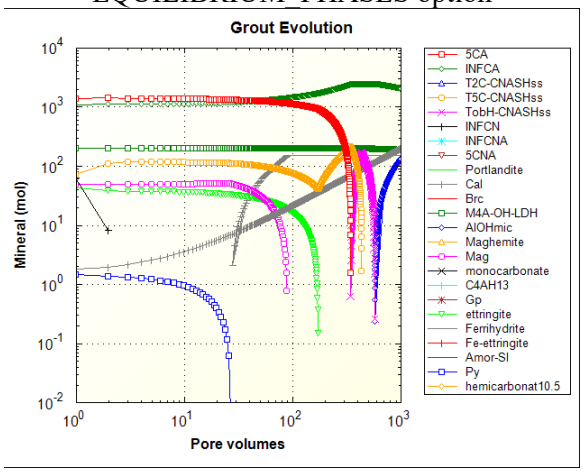

When salt solution is the mixing fluid (Figure 1), neither ettringite nor gypsum are observed in simulations, except for the case of partially hydrated dry binders and solid solution components treated as independent pure phases. In the latter case (Figure 1d), ettringite is initially present and disappears within 10 pore volume flushes. The high ionic strengths observed in the initial pore solutions fall below one molal after the first pore volume flush. When salt solution is diluted (except $NaSO_4$), ettringite is observed in the partially hydrated grouts and gradually disappears through dissolution (Figures 2c, d). For complete hydration and the SOLID_SOLUTIONS option, gypsum is initially present and disappears after two pore volumes (Figure 2a). Neither ettringite nor gypsum are present in the completely hydrated grout simulated with the EQUILIBRIUM_PHASES option (Figure 2b). When water is the mixing fluid (Figure 3), gypsum is observed for completely hydrated binders (Figure 3a, b) and ettringite for partially hydrated binders (Figure 3c, d). In each case, the sulfate phase gradually dissolves with pore volume exchanges.

To summarize, experimental observations and equilibrium chemistry simulations indicate that ettringite and/or gypsum formation in initially cured saltstone is not expected. Simulated saltstone variants prepared

with lower concentration salt solution or water may contain ettringite or gypsum initially, but these sulfate phases dissolve away with successive pore volume flushes. No ingrowth of expansive phases is observed in simulations. Degradation due to expansive phase formation has not been detected in physical saltstone samples stored for months to years (e.g., CBP-TR-2015-015, Rev. 1, Section 5.0). Thus, DOE continues to believe that sulfate attack on saltstone is not a significant degradation mechanism.

Static and dynamic (seismic) loading and settlement: K-ESR-Z-00008 investigated the potential for static and dynamic settlement of the SDU 7 design, which is applicable to SDUs 7 through 12. Estimated settlements due to static loading are:

- Heave during excavation: 0.4 inch
- Operations complete: 2 inches
- Closure Cap Complete: 3.5 inches
- 30 Years after Closure: 5 inches

Estimated dynamic settlements due to liquefaction and partial liquefaction and the compression of soft zones are:

- Liquefaction: 0.75 inch
- Soft Zone Settlement: 0.5 inch
- Total Dynamic Settlement: 1.25 inch

The combined static and dynamic settlement 30-years post-closure is 5 + 1.25 = 6.25 inches. Regarding differential settlement, K-ESR-Z-00008 states:

> "The differential static settlement is estimated ½ inch across a distance equal to the tank radius. The differential settlement resulting from liquefaction is estimated to be ¾ inch. The differential settlement resulting from the compression of soft zones is estimated to be ½ inch."

SDU 7 has been designed to withstand SRS SDC-2 (DOE-STD-1020-2012) and ANSI/AWWA D110-13 seismic loads per drawing C-C2-Z-00016. Considering the robust structural design of SDU 7 and minimal (<1 inch) differential settlements predicted, DOE believes settlement cracking of the saltstone monolith to be of low probability and limited extent while the concrete containment structure is sound. After the surrounding concrete structure has sufficiently degraded, damage to saltstone due to seismic events could be postulated because the structural integrity of the monolith in the absence of the concrete disposal cell has not been analyzed.

Early-age in-field observations: Potential degradation phenomena such as cracking due to thermal stresses and drying shrinkage are likely to occur in the near-term and be observable in the field prior to disposal unit closure. Video inspection of SDU 4 described in SRR-CWDA-2011-00105 indicates occasional cracks of indeterminate depth and extent. Thus, the saltstone monoliths in each disposal cell appear to largely intact and initial degradation appears to be minimal.

Probabilistic degradation model: Although the above supplementary information provides additional support for SDF PA assumptions (SRR-CWDA-2019-00001), saltstone degradation predictions are inherently uncertain. To support probabilistic sensitivity analysis and uncertainty quantification under *RSI-1: Combined Uncertainty of Flow Barriers*, the saltstone degradation fraction model is expanded herein

to accommodate the possibilities of an initially degraded state and/or abrupt degradation events, as depicted in Figure 4.

Figure 4: Generalized saltstone degradation model.

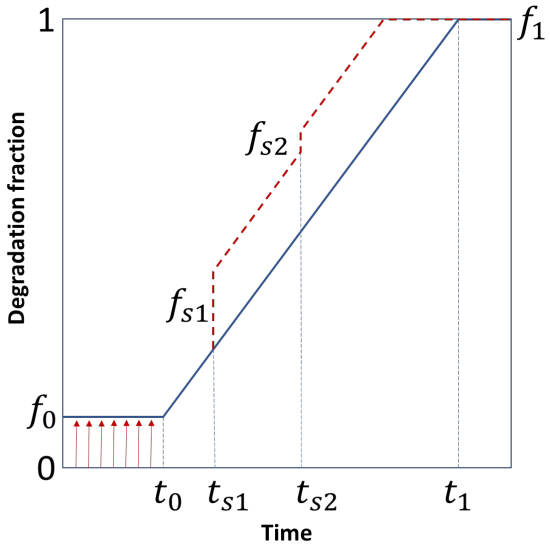

The degradation fraction, $f(t)$, is the volume fraction of the cementitious material that has become degraded, that is, the fraction of the total volume occupied by the end-member material representing the fully degraded state. Similarly, $1 - f(t)$ is the fraction of volume occupied by the end-member material representing the undegraded initial condition. The piecewise-linear curve depicted in Figure 4 representing only gradual degradation is

$$f(t) = f_0 + (f_1 - f_0) \cdot \frac{min[max(t, t_0), t_1] - t_0}{t_1 - t_0} \tag{1}$$

An initially degraded state occurs when $f_0 > 0$. The final state is assumed to be the fully degraded condition, $f_1 = 1$. An abrupt degradation (e.g., seismic) event at t_{si} can be accommodated by assuming a step increase, f_{si}, in the degradation fraction. The generalized function representing continuous degradation and discrete degradation events is

$$f(t) = min\left\{f_0 + (f_1 - f_0) \cdot \frac{min[max(t, t_0), t_1] - t_0}{t_1 - t_0} + \sum f_{si} H(t - t_{si}), f_1\right\} \tag{2}$$

where H is the Heaviside function: $H(x) = 0$ for $x < 0$ and $H(x) = 1$ for $x \geq 0$. The occurrence (t_{si}) and magnitude (f_{si}) of abrupt degradation events may be defined through random sampling. Figure 4 shows an example with two abrupt degradation events.

To generate random realizations of $f(t)$ within a probabilistic simulation, statistical distributions are required for:

- f_0, initial material condition

- f_s, fraction of damage from each abrupt event
- t_0, time degradation begins
- t_1, time of complete degradation
- t_s, time of each abrupt event.

Alternatively, reasonable (or expected) deterministic values can be assigned for less important parameters, while bounding (or more defensible) deterministic values assigned for more important variables.

In the sections that follow, statistical distributions are assigned to f_0, calcium solubility which influences t_1 for decalcification, f_s, and t_s. Deterministic values are assigned to t_0 and solid-phase calcium content which influences t_1. Finally, flow rate in the decalcification calculation for t_1 is conservatively set to the cover system infiltration rate, $I(t)$, which can be assigned a deterministic or probabilistic function based on SRR-CWDA-2021-00040.

Initial degradation, f_0: Any initial saltstone degradation is expected to take the form of discrete cracks/fractures. Suppose the hydraulic effects of a typical crack is represented by a surrogate 1.0-centimeter-thick seam of backfill soil, the end-member representing the fully degraded state. Then a crack spacing of 1 meter corresponds to f_0 = 0.01 for example. Based on these concepts and considering the observations described in SRR-CWDA-2011-00105, a triangular distribution for f_0 is proposed as shown in the probability distribution function (PDF) depicted in Figure 5. The minimum is f_0 = 0 or no initial degradation. The mode is f_0 = 0.003 or one crack approximately every 10 feet. The maximum is f_0 = 0.03 or one crack about every foot. The median value marked with a red dot is 0.01 or a crack spacing of 1.0 meters.

Figure 5: PDF for initial degradation state of saltstone.

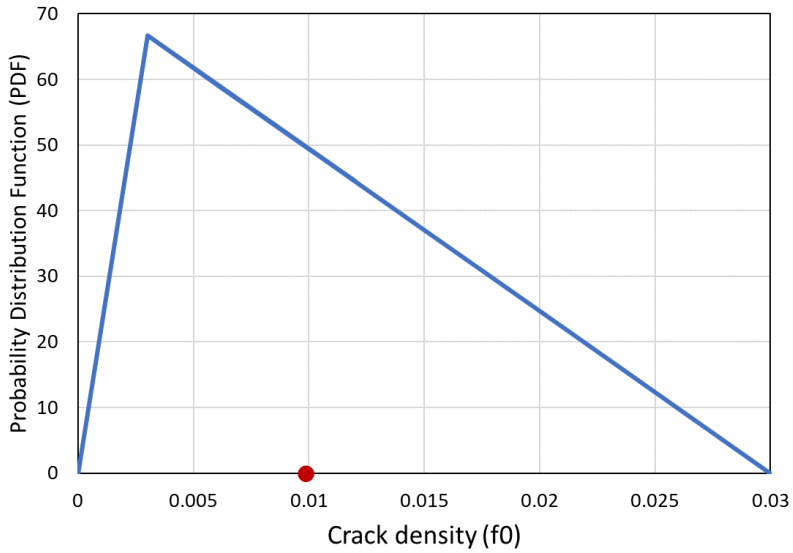

Degradation start time, t_0: Degradation of saltstone by decalcification occurs when roof concrete has fully degraded. For the SDU 7 Compliance Case t_0 = 1552 years, which is brief compared to the degradation period exceeding 10 million years. To avoid generating probabilistic distributions for concrete degradation, deterministic treatment of t_0 is proposed.

Degradation end time, t_1: Saltstone degradation by decalcification in the SDF PA (SRR-CWDA-2019-00001) is based on assumed hydraulic properties and gradients. While these assumptions are conservative (i.e., biased towards faster flow rates through saltstone as the material degrades) for the Central Scenario and most sensitivity cases considered, they might be non-conservative in a probabilistic study for certain combinations of parameters. Uncertainty in the decalcification degradation mechanism is most easily considered by adopting a bounding Darcy velocity. Flow through saltstone over time is effectively bounded by the cover system infiltration rate, $I(t)$, which can be varied in a deterministic or probabilistic manner (SRR-CWDA-2021-00040). Thus, a conservative estimate of the decalcification time t_1 is

$$\int_{t_0}^{t_1} I(t)dt = \frac{c_{Ca}}{c_{Ca^{++}}} h \tag{3}$$

where h is the height of saltstone, c_{Ca} is the amount of calcium in the solid phase per total volume, and $c_{Ca^{++}}$ is the average calcium solubility over time. Note that Equation (3) does not involve the hydraulic conductivity of saltstone or hydraulic gradients. Thus, the revised decalcification calculation is decoupled from hydraulic conductivity and gradients and takes no credit for saltstone conductivity likely diverting higher flows around the waste form.

A probabilistic variation is proposed for time-averaged Ca solubility. The solubility of calcium is estimated in the SDF PA (SRR-CWDA-2019-00001) to be approximately 0.002 mol/L based on $C\text{-}S\text{-}H$ gel dissolution. This estimate is supported by tank-fill grout simulations reported in SRR-CWDA-2021-00034. Ca solubility is bounded by about 0.02 mol/L, which occurs when portlandite is present in a cementitious material (e.g., SRR-CWDA-2021-00034, Section 6.2). Because portlandite is not expected in saltstone, 0.02 mol/L is a defensible upper bound. Long term calcium solubility is expected to decrease as the Ca/Si ratio in $C\text{-}S\text{-}H$ gel declines, to around 0.001 mol/L. This value can be taken as the lower bound for average solubility over time. The triangular distribution for $log10(c_{Ca^{++}})$ shown in Figure 6 reflects these three points of reference. The median of the log-triangular distribution depicted by a red dot is -2.5 or a Ca solubility of 0.0031 mol/L.

Figure 6: PDF for calcium solubility in saltstone.

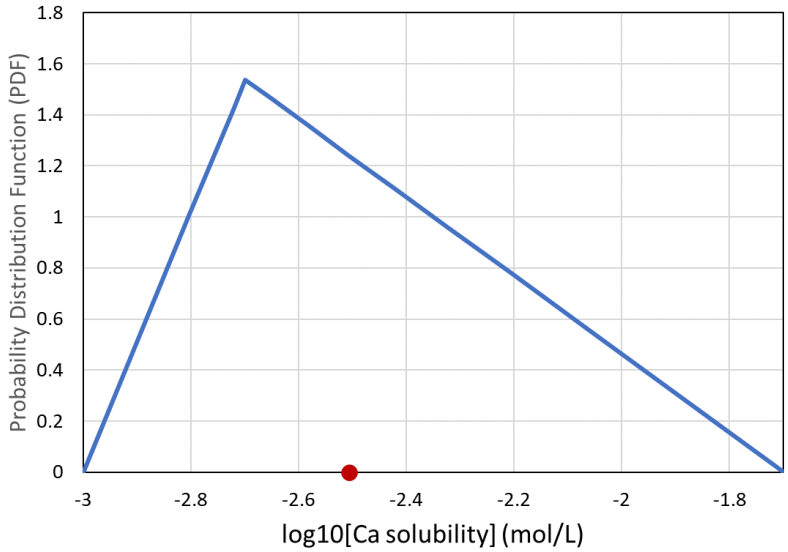

The amount of calcium in the solid phase is well known based on characterization of the dry ingredients, and c_{Ca} fixed at its deterministic Compliance Case value is proposed for RSI-1. Similarly, the height of saltstone h is considered a known value.

Seismic damage: As stated earlier, the structural integrity of the saltstone monolith in the absence of the surrounding concrete disposal cell has not been quantitatively analyzed. Thus, seismic damage to saltstone cannot be ruled out after the concrete containment structure has sufficiently degraded after a few thousand years, even though the monolith will be well protected compared to above-ground exposure. Regarding the latter, K-ESR-Z-00008 states "the project site is generally not susceptible to liquefaction, excepting isolated lenses at depth." To understand the risk significance of the SDF PA assumption that any post-closure earthquake(s) will not damage saltstone, consideration of abrupt seismic events is proposed for RSI-1 probabilistic analysis. The frequency of the design basis earthquake considered in K-ESR-Z-00008 is 0.0004/yr (2,500-year period). For RSI-1 simulations, instantaneous increases to the degradation fraction with an annual probability of 0.0004 is proposed, starting when the first SDU concrete component (roof, wall, floor) has fully degraded. Subsequent increases to the degradation fraction may be added in this manner until complete failure is achieved. Complete failure means the hydraulic properties of saltstone will be those of the surrounding backfill soil.

Effective hydraulic properties: As stated earlier, the degradation fraction $f(t)$ is the volume fraction of the end-member material representing the fully degraded state. For volume-based hydraulic properties such as porosity, the arithmetic average of the end-member porosities weighted by $f(t)$ is the effective porosity of the composite, partially degraded, material (e.g., SRNL-STI-2017-00525). For hydraulic conductivity, the appropriate average depends on the geometry of the intact and degraded materials, or more generally the nature of the spatial heterogeneity. In the context of the SDF PA (SRR-CWDA-2019-00001), this topic is discussed in SRNL-STI-2018-00077 Section 11, where geometric averaging is selected for computing the effective hydraulic conductivity of degraded cementitious materials. Further discussion of hydraulic conductivity averaging and uncertainty is provided here.

A general averaging method for effective conductivity K_e is (Ababou and Wood 1990)

$$K_e^p = \overline{K^p} \tag{4}$$

where $\overline{K^p}$ denotes the arithmetic average of K raised to the power p and $-1 \le p \le +1$. Special cases include:

arithmetic averaging: $p = +1$
geometric averaging: $p \to 0$
harmonic averaging: $p = -1$

The appropriate averaging scheme for degrading saltstone depends on how degradation evolves spatially. For decalcification evolving from the top down in a shrinking core manner, the intact and degraded end-member materials are distinct layers oriented perpendicular to flow. In this case, the harmonic average is appropriate. At the other end of the spectrum, cracks in early-age saltstone could focus flow along vertical fast-flow paths that accelerate local dissolution and promote further parallel fast-flow. Degradation proceeding in this fingered manner could be approximated by an arithmetic average for effective K. For deterministic modeling cases, DOE chose geometric averaging ($p \to 0$), which lies midway between harmonic and arithmetic averaging, as was recommended by Brown and Garrabrants (2017). As another point of reference, the effective saturated hydraulic conductivity of a 3D medium with isotropic

heterogeneity may be determined by averaging with $p = 1/3 \cong +0.33$ (e.g., Sanchez-Vila et al. 2006). Isotropic heterogeneity is consistent with a mixture of vertical and horizontal cracks, where the former might be initiated by thermal stresses and the latter by cold joints between saltstone pours. Considering the range of potential degradation geometries, a triangular distribution for the averaging power p is proposed to represent uncertainty in the effective hydraulic conductivity of degrading saltstone. As shown in Figure 7, the minimum, mode, and maximum values are -1, $+0.33$, and $+1$, respectively. The median value denoted by the red dot is $+0.15$.

Figure 7: PDF for averaging power, *p*.

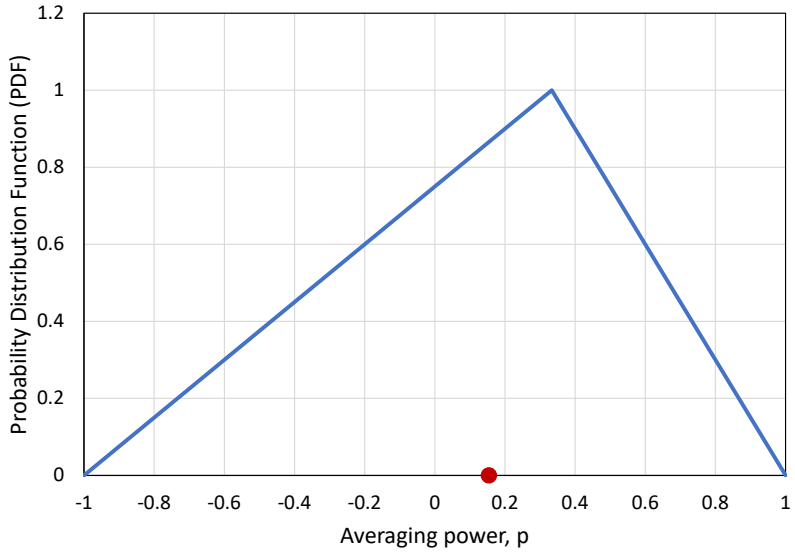

To summarize the latter portion of this memorandum, either a statistical distribution or deterministic value has been proposed for each component of the saltstone degradation function $f(t)$ and a statistical distribution assigned to the hydraulic conductivity averaging power p. These specifications are intended to support probabilistic analysis under *RSI-1: Combined Uncertainty of Flow Barriers* with the low hydraulic conductivity of saltstone being one of the barriers to flow and contaminant release.

References

Ababou, R. and E. F. Wood. *Comment on "Effective groundwater model parameter values: influence of spatial variability of hydraulic conductivity, leakance, and recharge" by J. J. Gomez-Hernandez and S. M. Gorelick*. Water Resources Research, v26, n8, 1843-1846. 1990.

ANSI/AWWA D110-13, *Wire- and Strand-Wound, Circular, Prestressed Concrete Water Tanks*, American Water Works Association, August 2018.

Brown, K.G., and Garrabrants, A., *Predicting the Hydraulic Conductivity over Time for Degrading Saltstone Vault Concrete – Task 5 (Subcontract Number SRRA110110)*, December 2017.

C-C2-Z-00016, *Z Area Saltstone Disposal Site, SDU 7 Tank Design General, General Structural Notes*, Savannah River Site, Aiken, SC, Rev. 3, October 2018.

CBP-TR-2015-015, Protière, Y., and E. Samson, *Cementitious Barriers Partnership Task 12 – Experimental Study; Experimental study of the concrete/saltstone 2-layer system*, DOE Cementitious Barriers Partnership, Rev. 1, November 2016.

DOE-STD-1020-2012, *DOE STANDARD: Natural Phenomena Hazards Analysis and Design Criteria for DOE Facilities*, U.S. Department of Energy, Washington DC, December 2012.

K-ESR-Z-00008, *Saltstone Disposal Unit 7 Geotechnical Investigation Report*, Savannah River Site, Aiken, SC, Rev. 0, November 2017.

Lothenbach, B., D.A. Kulik, T. Matschei, M. Balonis, L. Baquerizo, B. Dilnesa, G.D. Miron, and R.J. Myers, *Cemdata18: A chemical thermodynamic database for hydrated Portland cements and alkali-activated materials*, Cement and Concrete Research, 115, 472–506, 2019.

Nuclear Regulatory Commission, *Preliminary Review of the U.S. Department of Energy's Submittal of the 2020 Savannah River Site Saltstone Disposal Facility Performance Assessment*, letter from S. Koenick to J. Folk dated October 5, 2020.

Sanchez-Vila, X., A. Guadagnini, and J. Carrera, *Representative hydraulic conductivities in saturated groundwater flow*, Rev. Geophys., 44, RG3002, doi:10.1029/2005RG000169, 2006.

SRNL-STI-2012-00404, Denham, M.E. and M.R. Millings, *Evolution of Chemical Conditions and Estimated Solubility Controls on Radionuclides in the Residual Waste Layer during Post-Closure Aging of High-Level Waste Tanks*, Savannah River Site, Aiken, SC, Rev. 0, August 2012.

SRNL-STI-2014-00397, *X-ray Diffraction of Slag-based Sodium Salt Waste Forms*, Savannah River Site, Aiken, SC, Rev. 1, September 2014.

SRNL-STI-2017-00525, Flach, G.P., *Method for Modeling the Gradual Physical Degradation of a Porous Material*, Savannah River National Laboratory, Aiken, SC, Rev. 0, September 2017.

SRNL-STI-2018-00077, Flach, G.P., *Degradation of Saltstone Disposal Unit Cementitious Materials*, Savannah River National Laboratory, Aiken, SC, Rev. 1, August 2018.

SRR-CWDA-2011-00105, *Saltstone Disposal Facility Vault 4 Video Inspection Summary*, Savannah River Site, Aiken, SC, Rev. 0, July 2011.

SRR-CWDA-2019-00001, *Performance Assessment for the Saltstone Disposal Facility at the Savannah River Site*, Savannah River Site, Aiken, SC, Rev. 0, March 2020.

SRR-CWDA-2021-00034, *Chemical and Physical Evolution of Tank Closure Cementitious Materials*, Savannah River Site, Aiken, SC, Rev. 0, April 2021.

SRR-CWDA-2021-00040, *Evaluation of the Uncertainties Associated with the SDF Closure Cap and Long-Term Infiltration Rates*, Savannah River Site, Aiken, SC, Rev. 0, June 2021.

X-ESR-Z-00045, Mangold, J.E., *SDU Thermal Model Inputs*, Savannah River Site, Aiken, SC, Rev. 1, August 2019.

Appendix:
Nuclear Regulatory Commission Request for Supplemental Information #4, Saltstone Degradation

In a letter dated October 5, 2020, the Nuclear Regulatory Commission (NRC) requested information supplemental to the SDF PA regarding degradation of saltstone grout. This request is denoted *RSI-4: Saltstone Degradation* and reproduced below:

RSI-4	**Request:** To evaluate the risk significance of the hydraulic performance of saltstone, the NRC staff needs information about how the following issues affect saltstone degradation: (1) additional and coupled saltstone degradation mechanisms; (2) arithmetic averaging of hydraulic conductivity for degraded and intact saltstone; and (3) uncertainty in flow through the closure cap and engineered barriers above the disposal structures.
	Basis: In the PA, the DOE assumed that the saltstone grout would degrade by decalcification when water flows through saltstone. With extremely limited water flow through the closure cap (i.e., infiltration is reduced by approximately three orders of magnitude from natural infiltration), the LLDL, and underlying composite barrier, the saltstone is projected not to degrade appreciably in the timeframes analyzed in the PA. That is because of the combination of the long time to the projected complete degradation of saltstone (i.e., 17 million years) and the use of a geometric average to calculate the effective hydraulic conductivity of saltstone. The NRC staff is concerned that: (1) decalcification could occur more quickly than projected due to potentially greater-than-assumed infiltration (see both RSI-1 and RSI-2 above); (2) additional and coupled degradation mechanisms could result in more rapid degradation of saltstone than the DOE assumed in the PA; and (3) the use of a geometric average is not adequately supported and could significantly underestimate the effective hydraulic conductivity of degraded saltstone. For saltstone grout, the only degradation mechanism carried past the screening process into the PORFLOW model supporting the PA was advection-controlled decalcification. The assumptions about saltstone from Section 2.7.6 of the PA stated: • "The saltstone will be completely encapsulated within the concrete [disposal structures]. As such, no significant mechanical degradation is expected to influence the performance of saltstone. Similarly, due to the chemical characteristics of saltstone, it is not subject to sulfate attack or microbial induced degradation and, because saltstone has no rebar or steel embedded within it, it is also not subject to carbonation. Therefore, it is reasonable to assume that decalcification (i.e., dissolution and chemical leaching of calcium) is the primary mechanism of saltstone degradation." The NRC staff evaluated those characteristics in Appendix A of the May 18, 2019, NRC TRR, "Saltstone Waste Form Physical Degradation" (ADAMS Accession No. ML19031B221) and provided information on potential additional saltstone degradation mechanisms. In that TRR, the NRC staff described that mechanical degradation can still affect saltstone due to mechanisms such as: long-term drying shrinkage, settlement, and loading. With respect to chemical degradation, the NRC staff described the potential for expansive phase formation and the lack of the DOE support for excluding sulfate attack. The NRC staff also described an observation of microbial activity on cast stone, which is similar to saltstone. The alkalinity and high pH of saltstone do not appear to preclude microbial degradation, especially with successive pore volume flushes decreasing the alkalinity and salt content. Thermal degradation due to temporal and spatial thermal gradients also could occur. Furthermore, feedback between multiple degradation mechanisms could further increase the rate of degradation. The PA and its supporting documents did not provide information to: (1) refute other plausible degradation mechanisms; (2) demonstrate that the assumed

	degradation rate due to decalcification represented or exceeded the potential rate of degradation due to additional and coupled degradation mechanisms; or (3) demonstrate the risk significance of saltstone degradation. The DOE use of geometric averaging is not adequately supported because it depends on the assumption that flow is perpendicular to degraded layers. If saltstone does not degrade uniformly from top-to-bottom creating a uniform, horizontal layer of degraded saltstone, then the geometric average will not yield a reasonable effective hydraulic conductivity. Degradation of saltstone is likely to be non-uniform and may be caused by formation of preferential flow paths and localized decalcification or degradation caused by other mechanisms. Under a more-typical, non-uniform degradation front, flow would tend to be parallel to the path of flow, which is better represented by an arithmetic average. Using the arithmetic average is consistent with what the DOE previously used in the 2014 DOE SDF Special Analysis Document (ADAMS Accession No. ML15097A366), which stated: • "This [2014 DOE SDF Special Analysis Document] applies the more conservative approach of linear averaging, in part to compensate for departures from flow and transport perpendicular to the uniform degradation front." Although the DOE presented results for an accelerated cementitious materials degradation case in Section 5.8.2.4 of the PA, that case does not appear to have any appreciable impact on saltstone grout within 100,000 years and therefore does not provide any insight into what could happen if there is more water flow through saltstone. The DOE also tested the effects of a higher initial hydraulic conductivity for saltstone in Section 5.8.2.4 of the PA; but, the range of conductivities tested in that case is within the range of observed hydraulic conductivity values for intact saltstone, not degraded saltstone.
	Path Forward: Provide an analysis that: (1) provides risk insight into the effects of additional and coupled saltstone degradation mechanisms; (2) uses a more realistic arithmetic average for degraded and intact saltstone; and (3) is consistent with the response to RSI-1, RSI-2, and RSI-3 regarding uncertainty in flow through the closure cap and engineered barriers above the disposal structures. It would be useful if that analysis would include the volumetric flow rates, as shown in Figure 7.1.1 of the PA, for key materials (e.g., saltstone, roof, walls, joints, fast flow paths).